

5. G. T. Burstein, *ibid.*, **37**, 549 (1981).
6. D. R. Baer and M. T. Thomas, *J. Vac. Sci. Technol.*, **18**, 722 (1981).
7. A. Kawashima, K. Asami, and K. Hashimoto, *J. Non-Cryst. Solids*, **70**, 69 (1985).
8. P. Marcus and O. Oda, *Mem. Sci. Rev. Met.*, p. 715 (Nov. 1979).
9. R. B. Diegle, N. R. Sorensen, and G. C. Nelson, *This Journal*, **133**, 1769 (1986).
10. R. B. Diegle, N. R. Sorensen, C. R. Clayton, M. A. Helfand, and Y. C. Lu, *ibid.*, **135**, 1085 (1988).
11. M. Pourbaix, *Atlas of Electrochemical Equilibria in Aqueous Solutions*, National Association of Corrosion Engineers, Houston, TX (1974).
12. A. R. Brooks, C. R. Clayton, K. Doss, and Y. C. Lu, *This Journal*, **133**, 2459 (1986).
13. C. R. Clayton and Y. C. Lu, *ibid.*, **133**, 2465 (1986).
14. C. S. Fadley, *Prog. Surf. Sci.*, **16**, 275 (1984).
15. J. E. Castle and C. R. Clayton, *Corros. Sci.*, **17**, 7 (1977).
16. P. M. A. Sherwood, in *Practical Surface Analysis by Auger and Photoelectron Spectroscopy*, D. Briggs and M. P. Seah, Editors, Appendix 3, Wiley, London (1983).
17. J. R. Vilche and A. J. Arvia, in *Passivity of Metals*, R. P. Frankenthal and J. Kruger, Editors, p. 861, The Electrochemical Society Monograph Series, Princeton, NJ (1978).
18. W. Y. Ching, *Phys. Rev.*, **B34**, 2080 (1986).
19. P. Swift, *Surf. Intrfc. Anal.*, **4**, 47 (1982).
20. N. S. McIntyre, D. D. Johnston, L. L. Coatsworth, R. D. Davidson, and J. R. Brown, *ibid.*, **15**, 265 (1990).
21. T. J. Chuang, C. R. Brundle, and D. W. Rice, *Surf. Sci.*, **60**, 286 (1976); *ibid.*, **59**, 413 (1976).
22. MSDS, NaH₂PO₄H₂O

Electrical Conductivity Measurements of Binary Solutions of Molten Alkaline-Earth Fluorides

Kwang Bum Kim^a and Donald R. Sadoway*

Department of Materials Science and Engineering, Massachusetts Institute of Technology, Cambridge, Massachusetts 02139-4307

ABSTRACT

The electrical conductivities of binary solutions of molten MgF₂-CaF₂, MgF₂-SrF₂, MgF₂-BaF₂, CaF₂-SrF₂, CaF₂-BaF₂, and SrF₂-BaF₂ were measured by electrochemical impedance spectroscopy in a conductance cell comprising twin capillaries of pyrolytic boron nitride, movable tungsten electrodes, and a molybdenum crucible. In three of the systems, MgF₂-CaF₂, CaF₂-SrF₂, and SrF₂-BaF₂, the specific electrical conductivity was found to vary linearly with composition at constant temperature, while in the other three systems, MgF₂-SrF₂, MgF₂-BaF₂, and CaF₂-BaF₂, there were pronounced negative deviations from additivity. In a given binary system, the relative excess specific conductivity was found to vary parabolically with composition at constant temperature. In a homologous sequence the parabolic constant was proportional to the relative polarizability of the cations comprising the binary system.

As part of a systematic investigation of the physical properties of fluxes for use in electroslag welding of titanium, the electrical conductivities of binary solutions composed of alkaline-earth fluorides were measured. A new conductance cell was designed and constructed for the purpose of determining the electrical properties of highly conductive and very corrosive melts at temperatures as high as 1600°C. In a previous publication, conductivity data for one-component melts of BeF₂, MgF₂, CaF₂, SrF₂, and BaF₂ were reported¹. This paper presents the results for the binary solutions MgF₂-CaF₂, MgF₂-SrF₂, MgF₂-BaF₂, CaF₂-SrF₂, CaF₂-BaF₂, and SrF₂-BaF₂.

Literature

There are only two previous investigations of binary alkaline-earth fluoride melts. Voronin *et al.*² measured electrical conductivities of all six binaries studied in the present work. Ogino *et al.*³ measured solutions of CaF₂-MgF₂ and CaF₂-BaF₂.

Experimental

To avoid many of the problems with previous attempts to measure the electrical conductivities of molten alkaline-earth fluorides, a new experimental apparatus was designed and constructed¹. The heart of the apparatus is the conductance cell comprising twin capillaries made of pyrolytic boron nitride tubing (Union Carbide Corp., Cleveland, OH), movable tungsten electrodes, and a molybdenum crucible. Temperature was measured by a thermocouple, ASTM Type B, protected by a closed-one-end molybdenum tube (Rhenium Alloys Inc., East Elyria, OH) immersed in the melt. A carbon-block resistance furnace

heated the specimen which was positioned inside the cylindrical graphite heating element.

The instrumentation for electrochemical impedance spectroscopy consisted of a potentiostat (Solartron Model 1286 Electrochemical Interface, Schlumberger Instruments, Burlington, MA) driven by a waveform generator (Solartron Model 1255 Frequency Response Analyzer, Schlumberger Instruments, Burlington, MA) connected to a personal computer (PC-AT, IBM, Armonk, NY). Data acquisition and analysis were controlled by the computer using code written in house expressly for this investigation.

The value of the cell constant was determined by measuring the impedance of the cell containing pure NaCl and reconciling these data with the known specific conductivity of NaCl⁴. To complete the certification of the cell, the specific conductivity of KCl was calculated with the use of the cell constant determined with NaCl. Finally, this calculated value of the electrical conductivity of KCl was compared to that reported in the literature⁵. Each time a new cell was commissioned, as for example when it was fitted with new pyrolytic boron nitride tubes, the entire certification procedure was followed, *i.e.*, determination of the new cell constant with NaCl and subsequent measurement of the electrical conductivity of KCl.

The electrical conductivities of molten binary alkaline-earth fluorides were determined according to the same experimental procedure used in certifying the conductance cell. In the argon atmosphere of a glove box, binary mixtures were prepared from reagent grade salts (CERAC, Milwaukee, WI) exceeding 99.9% purity. Prior to melting, the specimen was transferred to the furnace chamber and treated by vacuum drying at 300°C for 12 h. Then argon gas, 99.995% pure (Matheson Gas Products, Gloucester, MA), was admitted to the furnace chamber where it blanketed the specimen for the duration of the experi-

* Electrochemical Society Active Member.

^a Present address: Department of Metallurgical Engineering, Yonsei University, Seoul, Korea.

Table I. Summary of electrical conductivity data.

Composition (X ₂ , mole fraction of the 2nd component)	a, Coefficient of Eq. 1	b, Coefficient of Eq. 1	s, Standard error of estimate of ln κ	r, Coefficient of correlation	Temperature range (°C)	n, No. of data points
CaF ₂ -SrF ₂						
0.00	2.823	1692	0.0011	0.9988	1468-1587	42
0.25	2.822	1763	0.0009	0.9983	1484-1580	31
0.50	2.780	1727	0.0008	0.9962	1509-1562	24
0.75	2.769	1740	0.0009	0.9979	1482-1582	37
1.00	2.711	1674	0.0011	0.9965	1531-1604	25
CaF ₂ -BaF ₂						
0.00	2.823	1692	0.0011	0.9988	1468-1587	42
0.25	2.757	1705	0.0011	0.9989	1438-1569	76
0.50	2.733	1747	0.0011	0.9988	1440-1560	56
0.75	2.713	1737	0.0013	0.9980	1472-1574	68
1.00	2.743	1726	0.0017	0.9953	1452-1550	28
SrF ₂ -BaF ₂						
0.00	2.711	1674	0.0011	0.9965	1531-1604	25
0.25	2.755	1784	0.0011	0.9978	1502-1610	37
0.50	2.777	1816	0.0012	0.9982	1503-1622	29
0.75	2.710	1694	0.0017	0.9954	1509-1608	26
1.00	2.743	1726	0.0017	0.9953	1452-1550	28
MgF ₂ -CaF ₂						
0.00	2.675	1825	0.0039	0.9967	1322-1577	47
0.25	2.729	1771	0.0017	0.9977	1452-1614	63
0.50	2.721	1680	0.0019	0.9960	1473-1597	35
0.75	2.748	1631	0.0021	0.9961	1450-1600	51
1.00	2.823	1692	0.0011	0.9988	1468-1587	42
MgF ₂ -SrF ₂						
0.00	2.675	1825	0.0039	0.9967	1322-1577	47
0.25	2.657	1829	0.0015	0.9960	1481-1570	34
0.50	2.633	1839	0.0013	0.9921	1502-1585	24
0.75	2.649	1746	0.0011	0.9977	1503-1580	16
1.00	2.711	1674	0.0011	0.9965	1531-1604	25
MgF ₂ -BaF ₂						
0.00	2.675	1825	0.0039	0.9967	1322-1577	47
0.25	2.714	2085	0.0029	0.9986	1325-1595	42
0.50	2.793	2260	0.0028	0.9992	1313-1586	46
0.75	2.742	1966	0.0032	0.9988	1320-1594	40
1.00	2.743	1726	0.0017	0.9953	1452-1550	28

ment. Before the first measurements were made, the specimen was held at 1600°C for 2 h to remove traces of volatile impurities.

Cell impedance was determined by applying an ac voltage across the electrodes and measuring the current response. The excitation voltage was sinusoidal, its dc bias set at zero, its amplitude fixed at 5 mV, and its frequency set sequentially at 50 values between 1 kHz and 100 kHz. At each temperature the entire frequency range was swept at least twice in order to acquire enough data to allow the determination of the solution resistance from the Nyquist plot. Then the electrodes were moved in order to change the interelectrode spacing. For more details about how the solution resistance was extracted from the cell impedance the reader is directed to the antecedent of this publication¹.

Results

The measured values of specific electrical conductivity for binary solutions of alkaline-earth fluorides have been fit by least squares regression to an Arrhenius-type equation of the form

$$\ln \kappa = a - b/T \quad [1]$$

where κ is in $\Omega^{-1} \text{cm}^{-1}$ and T is in Kelvins. The raw data are reported elsewhere⁶. For each composition, Table I presents the coefficients a and b as defined in Eq. 1; the standard error of estimate of $\ln \kappa$, s ; the coefficient of correlation, r ; the temperature range of investigation, and the number of data points, n .

Discussion

Figures 1, 2, and 3 show the concentration dependence of κ conveyed in terms of the isotherm at 1525°C. It is evident that these six binary systems fall into two categories,

which for the purposes of further discussion will be referred to as Category 1 and Category 2. In Category 1, consisting of MgF₂-CaF₂, CaF₂-SrF₂, and SrF₂-BaF₂, κ at constant temperature varies linearly with composition according to simple additivity. In Category 2, consisting of MgF₂-SrF₂, MgF₂-BaF₂, and CaF₂-BaF₂, κ at constant temperature is not linear in composition; instead, there are pronounced negative deviations from additivity. In fact, in

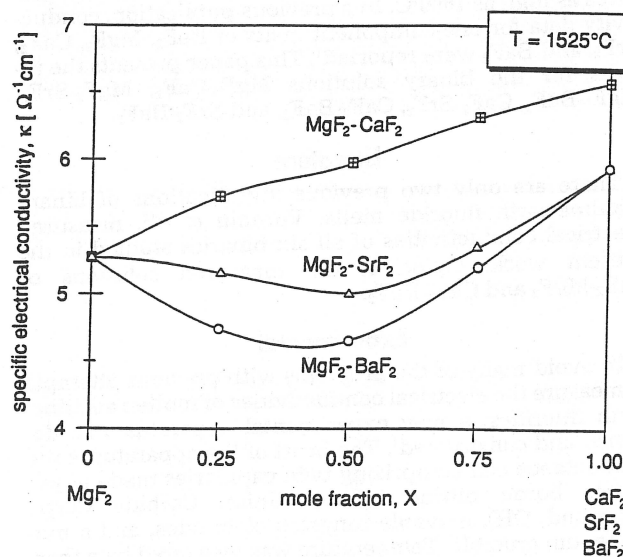


Fig. 1. Isothermal concentration dependence of specific electrical conductivity, κ , in the systems, MgF₂-CaF₂, MgF₂-SrF₂, and MgF₂-BaF₂, at 1525°C.

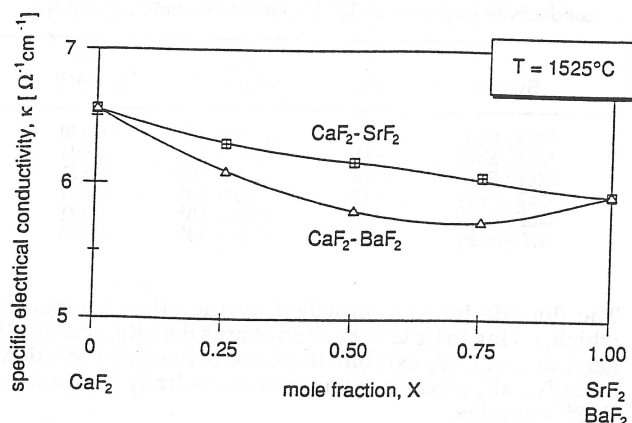


Fig. 2. Isothermal concentration dependence of specific electrical conductivity, κ , in the systems, $\text{CaF}_2\text{-SrF}_2$ and $\text{CaF}_2\text{-BaF}_2$, at 1525°C .

all three systems in Category 2, the minimum value of κ in the binary solutions is lower than κ of either of the two primary constituents.

For the most part there is good agreement with the earlier work by Voronin *et al.*² and by Ogino *et al.*³, i.e., the variation between the data sets from the three laboratories is typically less than 4% at a representative temperature of 1500°C . There are two exceptions. One of these has been described previously¹, namely, the 11% difference between the values of κ_{BaF_2} in this study and those measured by Voronin *et al.*² The other is in the $\text{MgF}_2\text{-CaF}_2$ binary where the measurements of Ogino *et al.*³ and those of the present study show κ to vary linearly with composition. In contrast, Voronin *et al.*² found pronounced negative deviation from additivity, a feature found in this study only in systems composed of cations with strong differences in charge density, i.e., Category 2.

The comparison of specific electrical conductivities suffers from the fact that κ is a practical unit representing the electrical current carrying capacity of a fixed volume of melt and thus is confounded by changes in density as well as changes in the electrical mobilities of the ions. More valuable from a theoretical standpoint is the molar conductivity, Λ_m , which is compensated so as to represent a fixed number of chemical entities, if not a fixed number of charge carriers in the most ideal cases. In this work the molar electrical conductivity is defined as

$$\Lambda_m = \kappa V_m \quad [2]$$

where V_m is the molar volume.

Thus, to transform the measured values of κ into Λ_m requires knowledge of the concentration and temperature dependences of V_m , typically derived from density measurements. Unfortunately, density data are available for only three of the six binary systems studied in the present investigation: $\text{MgF}_2\text{-CaF}_2$, $\text{CaF}_2\text{-SrF}_2$, and $\text{CaF}_2\text{-BaF}_2$.⁷ In these three systems the molar volume of binary solutions conforms to the rules of additivity: the maximum deviation was 1.4% in $\text{CaF}_2\text{-BaF}_2$. In the light of this information, the molar volumes of the three binary systems for which there were no data were estimated by applying the rules of additivity. In the $\text{SrF}_2\text{-BaF}_2$ system this approximation is expected to be valid. In the $\text{MgF}_2\text{-SrF}_2$ and $\text{MgF}_2\text{-BaF}_2$ systems, however, strict adherence to additivity is not expected, owing to the tendency for MgF_2 to form complexes. At the same time, the pronounced deviation from additivity in the Λ_m isotherms is expected to exceed by far that attributable to nonlinearities in V_m . Evidence for this can be found in the $\text{CaF}_2\text{-BaF}_2$ system for which there is a complete set of conductivity and density data. At 1525°C for the solution composed of equimolar amounts of CaF_2 and BaF_2 the maximum deviation in Λ_m is -5.2% while the maximum deviation in V_m is only -1.4% .

Isotherms of Λ_m behave much the same as isotherms of κ . In the $\text{MgF}_2\text{-CaF}_2$, $\text{CaF}_2\text{-SrF}_2$, and $\text{SrF}_2\text{-BaF}_2$ systems, Λ_m varies linearly with composition according to simple additivity. In the $\text{MgF}_2\text{-SrF}_2$, $\text{MgF}_2\text{-BaF}_2$, and $\text{CaF}_2\text{-BaF}_2$ sys-

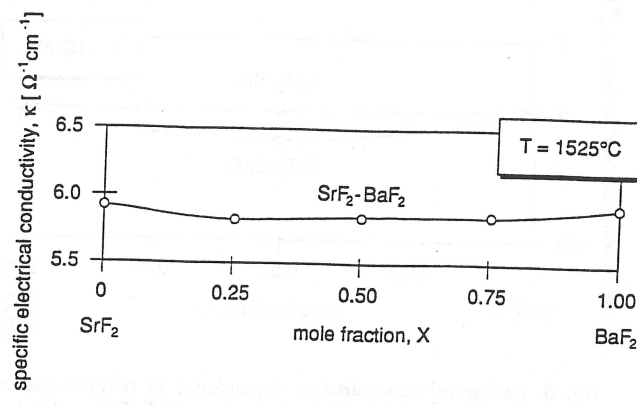


Fig. 3. Isothermal concentration dependence of specific electrical conductivity, κ , in the system, $\text{SrF}_2\text{-BaF}_2$, at 1525°C .

tems, there are pronounced negative deviations. To elucidate the precise nature of the isothermal concentration dependence of molar conductivity, Λ_m values were rationalized to compensate for differences in the absolute value of Λ_m between the various pure components. This was accomplished by viewing the results for binary melts in terms of relative excess molar electrical conductivity, Λ_m^{rel} , defined as

$$\Lambda_m^{\text{rel}} = (\Lambda_m^{\text{xs}}/\Lambda_m^{\text{id}}) \times 100\% \quad [3]$$

The excess molar electrical conductivity, Λ_m^{xs} , is the difference between the measured value of Λ_m in a binary solution and the value calculated on the basis of a linear combination of the values of Λ_m of the pure components weighted by mole fraction

$$\Lambda_m^{\text{xs}} = \Lambda_m - (\Lambda_{m1} X_1 + \Lambda_{m2} X_2) = \Lambda_m - \Lambda_m^{\text{id}} \quad [4]$$

where Λ_{mi} is the molar electrical conductivity of pure molten i at the same temperature as the binary solution, and X_i is the mole fraction of i in the binary solution. The term in parentheses can also be thought of as representing the value of Λ_m in a strictly ideal binary solution. Thus, in a sense, Λ_m^{xs} measures absolute deviation from additivity.

The concentration dependence of Λ_m^{rel} is shown in Fig. 4, 5, and 6 which plot isotherms at 1525°C for the same systems shown in Fig. 1, 2, and 3, respectively. For the three systems in Category 2 there appears to be a parabolic dependence of Λ_m^{rel} on composition. The solid lines in Fig. 4,

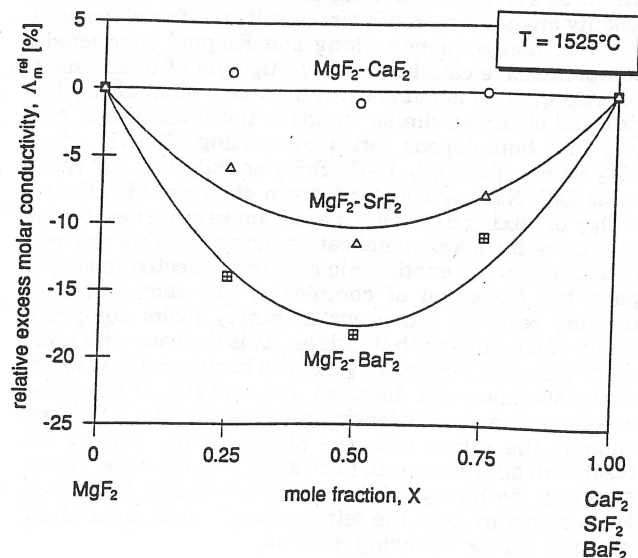


Fig. 4. Isothermal concentration dependence of relative excess molar electrical conductivity, Λ_m^{rel} , in the systems, $\text{MgF}_2\text{-CaF}_2$, $\text{MgF}_2\text{-SrF}_2$, and $\text{MgF}_2\text{-BaF}_2$, at 1525°C .

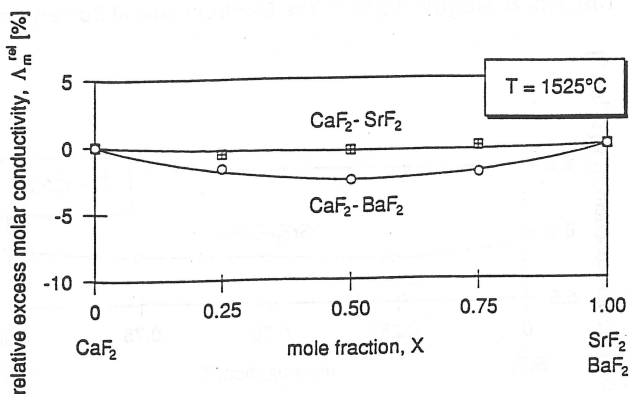


Fig. 5. Isothermal concentration dependence of relative excess molar electrical conductivity, Δ_m^{rel} , in the systems, $\text{CaF}_2\text{-SrF}_2$ and $\text{CaF}_2\text{-BaF}_2$, at 1525°C .

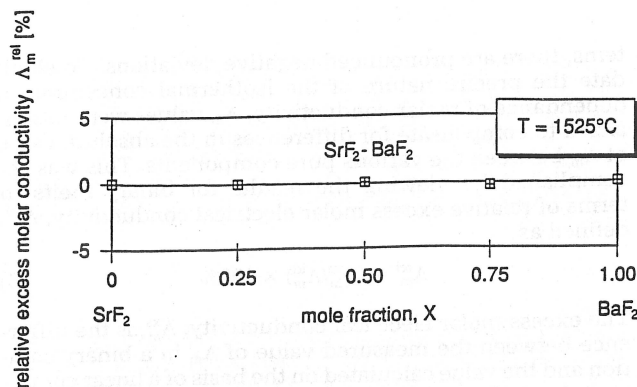


Fig. 6. Isothermal concentration dependence of relative excess molar electrical conductivity, Δ_m^{rel} , in the system, $\text{SrF}_2\text{-BaF}_2$ at 1525°C .

5, and 6 represent the least squares regressions of the data to an equation of the form

$$\Delta_m^{\text{rel}} = \beta X_1 X_2 = \beta X_1 (1 - X_1) \quad [5]$$

Table II gives the value of β at 1525°C for each binary system.

It is evident that the deviation from ideality in the transport properties of these binary solutions, as represented by Δ_m^{rel} , is to some extent correlated with the deviation from ideality in the thermodynamic properties of these binary solutions. The three systems exhibiting near ideal behavior are composed of consecutive pairs of salts in the homologous sequence: MgF_2 , CaF_2 , SrF_2 , BaF_2 . In contrast, the three systems exhibiting pronounced deviation from ideality are composed of pairs of salts not found consecutively in that sequence. Hong and Kleppa⁸ conducted a comprehensive calorimetric investigation of binary melts consisting of an alkaline-earth fluoride and an alkali fluoride and observed similar trends in the enthalpies of mixing. In a homologous series comprising $\text{MF}_2\text{-AF}$, where MF_2 represents MgF_2 , CaF_2 , SrF_2 , or BaF_2 and AF represents LiF , NaF , or KF , for a given choice of MF_2 , the enthalpy of mixing decreases, i.e., becomes more negative, as the size of the alkali-metal cation increases. This has been explained by the exothermic reaction expected to accompany the formation of complexes. The same complex-forming reaction can occur in binary melts comprised solely of alkaline-earth fluorides. As is the case with melts of the general formula, $\text{MF}_2\text{-AF}$, in a binary melt consisting of the alkaline-earth fluorides, AF_2 and BF_2 , if the difference in cation charge density between A^{2+} and B^{2+} is large enough, the cation with the higher charge density will react with fluoride ions to form anionic complexes. For example, in the binary solutions, $\text{MgF}_2\text{-SrF}_2$ and $\text{MgF}_2\text{-BaF}_2$, MgF_2 reacts to form the tetrahedrally coordinated MgF_4^{2-} complex via the following reaction

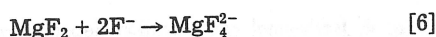


Table II. Least squares regression of relative excess molar electrical conductivity isotherms at 1525°C to the equation $\Delta_m^{\text{rel}} = \beta X_1 X_2$.

System	β (%)	$\Delta\rho_q$ (C cm^{-3})	α^{rel} ($(\text{nm})^{-2}$)
$\text{MgF}_2\text{-CaF}_2$	-0.45	1.29×10^5	0.159
$\text{MgF}_2\text{-SrF}_2$	-41	1.58×10^5	0.404
$\text{MgF}_2\text{-BaF}_2$	-70	1.74×10^5	0.621
$\text{CaF}_2\text{-SrF}_2$	-3.3	2.99×10^4	0.007
$\text{CaF}_2\text{-BaF}_2$	-20	4.54×10^4	0.131
$\text{SrF}_2\text{-BaF}_2$	-0.05	1.55×10^4	0.025

The fluoride ions are provided by the other component which, owing to its lower cation charge density, acts as a ligand donor. CaF_2 exhibits the same behavior in solutions of $\text{CaF}_2\text{-BaF}_2$ where it forms the tetrahedrally coordinated CaF_4^{2-} complex.

In a previous publication from this laboratory it was shown that for the pure alkaline-earth fluorides there is a correlation between the molar conductivity, Δ_m , and the charge density of the cation, ρ_q . Accordingly, values of β were plotted as a function of the difference in cation charge density, $\Delta\rho_q$, where ρ_q is obtained from

$$\rho_q = q_{A^{2+}} / (4/3 \pi r^3) \quad [7]$$

The charge on the alkaline-earth metal cation, $q_{A^{2+}}$, is constant at $2e_p$ or 3.2×10^{-19} C. In the absence of structural data for these melts, the ionic radius, r , in Eq. 7 was approximated by Shannon's effective ionic radius, which can be thought of as a crystal radius modified to reflect a number of matrix effects, most notably crystal structure⁹. Care was taken to choose values of the effective ionic radius determined for the same coordination number, in this case, 6. Values of $\Delta\rho_q$ for each of the six binary systems of this study were calculated on this basis and are reported in Table II. While some trends were evident, (for example, the values of β for the three binary systems, $\text{MgF}_2\text{-CaF}_2$, $\text{MgF}_2\text{-SrF}_2$, and $\text{MgF}_2\text{-BaF}_2$, appear to lie on the same line) the correlation of the data taken as a whole was poor. Correlations between β and other structural parameters were sought. One such parameter was the relative ionic potential¹⁰ of the two cations, ΔIP , defined as

$$\Delta IP = q_1/r_1 - q_2/r_2 \quad [8]$$

where q_i and r_i are the charge and radius of cation, i , respectively. Another such parameter was the so-called size parameter, δ_{12} , defined in the conformational solution theory of Reiss *et al.*¹¹ as

$$\delta_{12} = 1/d_1 - 1/d_2 \quad [9]$$

where d_k is the characteristic interionic distance in the pure melt, k . As was the case with the difference in cation charge density, $\Delta\rho_q$, some trends were evident, but no conclusions could be drawn.

In a study of the electrical conductivity of binary molten alkali chloride systems Zuca and Olteanu¹², applying concepts enunciated by Lumsden¹³, found that the deviations from additivity could be explained in terms of polarization of the common anion by cations of different sizes. To test the extent to which differential polarizability is important in binary molten alkaline-earth fluoride system, the values of β were plotted against the relative polarizability, α^{rel} , and the results are shown in Fig. 7. α^{rel} is a parameter defined in the present investigation as

$$\alpha^{\text{rel}} = \{1/(\tau_{\text{AF}_2} - d)^2 - 1/(\tau_{\text{BF}_2} + d)^2\} \quad [10]$$

where τ_{AF_2} and τ_{BF_2} are the interionic separations in the pure salts, AF_2 and BF_2 , respectively, and d is the correction defined by Sternberg and Herdlicka¹⁴ as the change in interionic separation attributable to fitting cations of different sizes around a common anion. The value of d is computed by the relation

$$d = 0.1274 (\tau_{\text{AF}_2} - \tau_{\text{BF}_2}) / \tau_{\text{F}^-} \quad [11]$$

α^{rel} has units of $(\text{nm})^{-2}$.

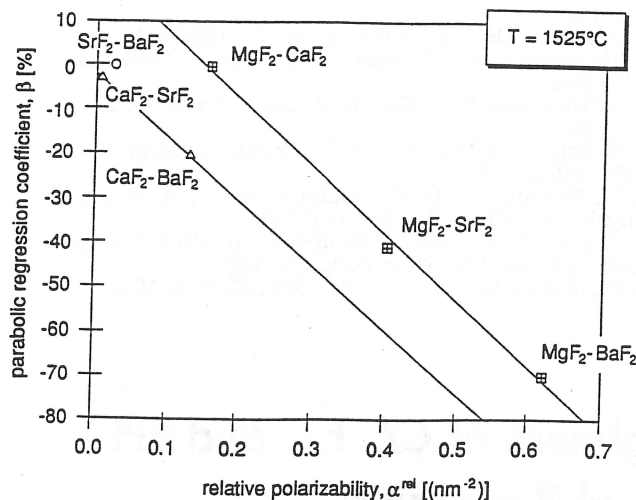


Fig. 7. Isothermal dependence of the parabolic regression constant, β , on the relative polarizability, α^{rel} , at 1525°C.

Figure 7 also reveals some interesting trends in the behavior of the parameter β along a homologous sequence. First, the line through $\text{MgF}_2\text{-CaF}_2$, $\text{MgF}_2\text{-SrF}_2$, and $\text{MgF}_2\text{-BaF}_2$, and the line through $\text{CaF}_2\text{-SrF}_2$ and $\text{CaF}_2\text{-BaF}_2$ have slopes differing by only 5%. Second, the line through $\text{MgF}_2\text{-SrF}_2$ and $\text{CaF}_2\text{-SrF}_2$ and the line through $\text{MgF}_2\text{-BaF}_2$ and $\text{CaF}_2\text{-BaF}_2$ have slopes differing by only 3%. Third, the data point for $\text{SrF}_2\text{-BaF}_2$ does not appear to lie on any of these lines. Taken as a set, these observations are in conformity with the hypothesis that in binary solutions of $\text{MgF}_2\text{-SrF}_2$ and $\text{MgF}_2\text{-BaF}_2$, MgF_2 reacts to form the MgF_4^{2-} complex and that in solutions of $\text{CaF}_2\text{-BaF}_2$, CaF_2 reacts to form the CaF_4^{2-} complex, according to Eq. 6. Furthermore, it appears not only that the stability of the complex increases with the size of the ligand donor (as expected), but that the change in stability of MgF_4^{2-} from $\text{MgF}_2\text{-SrF}_2$ to $\text{MgF}_2\text{-BaF}_2$ is the same as the change in stability of CaF_4^{2-} from $\text{CaF}_2\text{-SrF}_2$ to $\text{CaF}_2\text{-BaF}_2$. In the $\text{SrF}_2\text{-BaF}_2$ system, to the extent that complex formation occurs it does not have a measurable effect on the electrical conductivity, and thus the behavior of this binary system is similar to that of binary alkali fluorides¹⁵. Finally, while the concept of relative polarizability is helpful in following trends within a homologous sequence, it is necessary to invoke the concept of complex formation to explain why the value of β for the $\text{CaF}_2\text{-BaF}_2$ system is substantially negative while that of the $\text{MgF}_2\text{-CaF}_2$ system is effectively zero in spite of the fact that the relative polarizability of Mg-F-Ca far exceeds that of Ca-F-Ba.

In a previous publication from this laboratory it was shown that for the pure alkaline-earth fluoride melts there is a correlation between the molar conductivity, Λ_m , and the charge density of the cation, ρ_q ¹. In contrast, for binary solutions this relationship was found not to hold. Instead, there were pronounced negative deviations from the least squares regression line fitting Λ_m to $\ln \rho_q$. In this assessment, use of Eq. 7 to calculate the cation charge density of a binary melt required that an effective cation radius, τ_{eff} , be defined. A Vegard's law-type expression was adopted, i.e., in a binary melt consisting of the alkaline-earth fluorides, AF_2 and BF_2 , in the molar proportions, X_{AF_2} and X_{BF_2}

$$\tau_{\text{eff}} = \tau_{\text{A}^{2+}} X_{\text{AF}_2} + \tau_{\text{B}^{2+}} X_{\text{BF}_2} \quad [12]$$

It has also been shown in a previous publication from this laboratory¹ that the expression for the limiting equivalent ionic conductance as derived by the theory of transition states for use in dilute aqueous electrolytes¹⁶ can be adapted to represent the molar conductivity of a molten salt to the extent that the use of such an expression serves to identify the important parameters and the functional relationships between them. This is justified provided that electrical conduction in all the melts under consideration is dominated by the same ion. Voronin *et al.*,¹⁷ have argued that trends in the values of both molar conductivity and

viscosity in the alkaline-earth fluorides are consistent with electrical conduction predominantly by the fluoride ion. This being so, one can make the following crude approximation for Λ_m

$$\Lambda_m = 1/6 (z_{\text{eff}} e_0 F/h) L_{\text{eff}}^2 \exp(\Delta S^*/R) \exp(-\Delta H^*/RT) \quad [13]$$

where z_{eff} is the effective valence of the dominant charge carrier, L_{eff} is the effective jump distance, and ΔS^* and ΔH^* are the entropy and enthalpy of ion movement, respectively. Equation 13 can be rewritten in the form

$$\Lambda_m = \text{constant} \times L_{\text{eff}}^2 \exp(-\Delta H^*/RT) \quad [14]$$

The effective jump distance is expected to scale with the cube root of the molar volume, V_m . The enthalpy of activation must be related to the bonding energy of the melt which is approximated as the coulombic attraction energy between nearest neighbor ions. Thus, Eq. 14 can be expressed as

$$\Lambda_m = \text{constant} \times V_m^{2/3} \exp(k_c E_c/k_B T) \quad [15]$$

where k_c is a constant, E_c is the coulombic attraction energy between the fluoride anion and an alkaline-earth cation, and k_B is the Boltzmann constant. Furthermore

$$E_c = z_+ z_- e_0^2 / (4\pi\epsilon_0\epsilon_r) \times d \quad [16]$$

where ϵ_0 and ϵ_r are the permittivity of free space and relative permittivity of the molten salt, respectively, and d is the interionic distance between the anion and cation in the melt. A relative permittivity value of 3 for molten fluorides¹⁸ was used to calculate E_c . Studies of the structure of molten alkali halides by radial distribution function¹⁹ show that the nearest neighbor distance in the liquid is slightly smaller than that of the crystal, yet molar volume increases upon melting. In view of this, the interionic distance, d , was approximated by the sum of the Shannon effective ionic radii of the alkaline-earth metal cation and the fluoride anion.⁹ As was the case with the calculation of the cation charge density, selected values of the effective ionic radius at a constant coordination number of 6 were used.

Least-squares regression of the data for the four pure melts, MgF_2 , CaF_2 , SrF_2 , and BaF_2 , showed good correlation between $\ln \Lambda_m$ and $\ln \{V_m^{2/3} \times \exp(E_c/k_B T)\}$ at 1525°C¹. In contrast, for binary solutions this relationship was found not to hold; instead, there were pronounced negative deviations. It does not appear that there is an easily recognizable correlation between the electrical conductivity of pure alkaline-earth fluoride melts and binary solutions comprising them.

Acknowledgments

The authors gratefully acknowledge the following people and agency: Professor G. J. Janz, Molten Salts Data Center, Rensselaer Polytechnic Institute, Troy, NY, for providing reference grade NaCl and for sharing rare manuscripts containing raw data; Professor V. D. Prisyazhnyi, Institute of General and Inorganic Chemistry, Ukrainian Academy of Sciences, Kiev, for helpful discussions about experimental technique and interpretation of results; Guenther Arndt for technical assistance in the construction of the apparatus; Dr. Andrew Block-Bolten and James Landers for assistance in designing and testing earlier prototypes of cells and furnaces; the U. S. Office of Naval Research (ONR), Contract No. N00014-82-K-0564, for financial support of this investigation.

Manuscript submitted Oct. 22, 1992; revised manuscript received April 6, 1992.

Massachusetts Institute of Technology assisted in meeting the publication costs of this article.

REFERENCES

1. K. B. Kim and D. R. Sadoway, *This Journal*, **139**, 1027 (1992).
2. B. M. Voronin, V. D. Prisyazhnyi, K. K. Khizhnyak, V. N. Zamkov, and Yu. K. Novikov, *Ukr. Khim. Zh.*, **53**, 480 (1987).
3. K. Ogino, H. Hashimoto, and H. Hara, *Tetsu To Ha-*

- gane, 64, 225 (1978).
4. H. H. Emons and G. Brautigam, Submitted to Molten Salts Standard Program, Molten Salts Data Center, Rensselaer Polytechnic Institute, Troy, NY (1976).
 5. E. R. Van Artsdalen and I. S. Yaffe, *J. Phys. Chem.*, **59**, 118 (1955).
 6. K. B. Kim, Ph.D. Thesis, Massachusetts Institute of Technology, Cambridge, MA (1991).
 7. S. Hara, H. Shibaike, and K. Ogino, *ISIJ Int.*, **30**, 298 (1990).
 8. K. C. Hong and O. J. Kleppa, *J. Phys. Chem.*, **82**, 1596 (1978).
 9. R. D. Shannon, *Acta Crystallogr. A.*, **32**, 751 (1976).
 10. G. H. Cartledge, *J. Am. Chem. Soc.*, **50**, 2855 (1928).
 11. H. Reiss, J. L. Katz, and O. J. Kleppa, *J. Chem. Phys.*, **36**, 144 (1962).
 12. S. Zuca and M. Olteanu, *Rev. Roum. Chim.*, **15**, 357 (1970).
 13. J. Lumsden, *Discuss. Faraday Soc.*, **32**, 138 (1961).
 14. S. Sternberg and C. Herdlicka, *Rev. Roum. Chim.*, **13**, 13 (1968).
 15. J. L. Holm and O. J. Kleppa, *J. Chem. Phys.*, **49**, 2425 (1968).
 16. S. B. Brummer and G. J. Hills, *Trans. Faraday Soc.*, **57**, 1816 (1961).
 17. B. M. Voronin, V. D. Prisyazhnyi, and K. K. Khizhnyak, *Ukr. Khim. Zh.*, **46**, 584 (1980).
 18. G. J. Janz, *Molten Salts Handbook*, pp. 356-357, Academic Press, Inc., New York, NY (1967).
 19. K. Furukawa, *Discuss. Faraday Soc.*, **57**, 1816 (1961).

Dependence of Surface Microroughness of CZ, FZ, and EPI Wafers on Wet Chemical Processing

M. Miyashita, T. Tusga, K. Makihara, and T. Ohmi*

Department of Electronics, Faculty of Engineering, Tohoku University, Aoba, Sendai 980, Japan

ABSTRACT

The effect of the wet chemical cleaning process on the surface microroughness of Si wafers was studied, using CZ, FZ, and EPI wafers. It has been shown that the surface microroughness affects the dielectric breakdown characteristics of the oxide: the dielectric breakdown of the oxide degrades as the microroughness of the Si substrate increases. The microroughness on the Si substrate surface and the oxide surface was evaluated with a scanning tunneling microscope (STM) and an atomic force microscope (AFM). The surface microroughness was found to increase in wet chemical processing, in particular in $\text{NH}_4\text{OH}-\text{H}_2\text{O}_2-\text{H}_2\text{O}$ cleaning (APM cleaning). It has been shown that the microroughness does not increase at all if the NH_4OH mixing ratio in $\text{NH}_4\text{OH}-\text{H}_2\text{O}_2-\text{H}_2\text{O}$ solution is suppressed at a low level: $\text{NH}_4\text{OH}-\text{H}_2\text{O}_2-\text{H}_2\text{O}=0.05:1:5$ (conventional mixing ratio is 1:1:5), and the room temperature ultrapure water rinsing is introduced right after the APM cleaning. At the same time, the APM cleaning with its NH_4OH mixing ratio suppressed at the low level has been found very effective to remove particles and metallic impurities from the Si surface. The increase of microroughness due to the APM cleaning varies among the wafer types; little increase is observed on EPI wafer but significant increase is observed on CZ and FZ wafers. It has been found, however, that the CZ and FZ wafers which go through the wet oxidation at 1000°C for over 4 h, can suppress the increase of microroughness in the APM cleaning at almost the same level as the EPI wafer. This because the interstitial Si atoms generated in the wet oxidation fill the Si vacancy. In the case of the n-type CZ wafer, the surface microroughness is also observed to increase in the DHF cleaning. It has been revealed the addition of H_2O_2 of over 0.5% to the DHF solution can completely suppress this microroughness increase.

In the manufacturing process of sub-micron and deep sub-micron (ULSI) devices, it has been pointed out that the cleanliness of the substrate surface is the key factor in terms of the device performance and the reliability: the ultraclean wafer surface must be free from particles, organic impurities, metallic impurities, native oxide, adsorbed impurity molecules, and surface microroughness^{1,2}. The conventional cleaning process has been based upon the concept of the RCA cleaning which is efficient in removing such contaminants on the substrate surface as particles, organic materials, and metallic impurities³⁻⁵.

Meanwhile it has been revealed that if water and oxygen coexist, the native oxide immediately grows on the Si surface either in air or in the ultrapure water⁶. When the Si surface is covered with native oxide, the process quality, in particular the quality in the low-temperature process, gets extremely degraded⁷. Therefore, the introduction of the nitrogen-gas-sealed closed system concept has been proposed which completely prevents the native oxide from growing on the Si surface⁸. Furthermore, the gas phase cleaning technology has already been established: HF gas diluted with nitrogen gas is employed to selectively remove the native oxide without damaging other oxide films⁹.

As the device dimension is getting smaller, the device will be composed of thinner oxides and shallower junctions. Consequently, the effect of the surface microroughness on surface will become more critical in terms of the device performance and the reliability. The surface micro-

roughness on the substrate is caused by the cleaning process employing alkali solutions such as the APM cleaning. It has been proposed to reduce the mixing ratio of NH_4OH in the APM cleaning from the conventional level of 1:1:5 to a new level of 0.25:1:5¹⁰. Recently, the surface microroughness on the Si substrate and the thin oxide film was evaluated with a scanning tunneling microscope (STM) and an atomic force microscope (AFM) to reveal the influence of the surface microroughness on the electrical characteristics such as the dielectric breakdown (E_{BD}) and charge to breakdown (Q_{BD})¹¹⁻¹³.

In the above-mentioned studies, the surface microroughness was carefully evaluated to find out the effect of each cleaning process in the wet chemical process on the surface conditions of CZ, FZ, and EPI wafers. The surface smoothness gets deteriorated in the APM cleaning process: with the conventional mixing ratio of $\text{NH}_4\text{OH}:\text{H}_2\text{O}_2:\text{H}_2\text{O}=1:1:5$ the surface microroughness shows the significant increase. When the mixing ratio of the APM cleaning is changed to $\text{NH}_4\text{OH}:\text{H}_2\text{O}_2:\text{H}_2\text{O}=0.25:1:5$ and, after the APM cleaning, the room temperature ultrapure water rinsing adsorbed particles and metallic impurities can be effectively removed without the surface microroughness increase.

Meanwhile, it has been revealed that the surface microroughness strongly depends on the crystallinity, in particular the point defects including Si vacancy and interstitial Si and the oxygen concentration. In the case of the CZ wafer, the surface microroughness shows a sharp increase immediately after starting the cleaning. On the other hand, in the case of the FZ wafer, the surface microroughness

* Electrochemical Society Active Member.